Mass scattering efficiency and hygroscopic growth assumptions used to reconstruct light extinction coefficients using IMPROVE Equation 3.

J. L. Hand

May 2026

1. Introduction

Light extinction occurs in the atmosphere when incident light is attenuated by the scattering and absorption of light from particles and gases in the layer through which it travels. The Beer-Lambert law describes the fractional reduction in intensity (F) of incident flux (F_o) through a layer of thickness (z) as shown in Equation 1, where b_{ext} is the light extinction coefficient:

$$\frac{F}{F_o} = \exp(-b_{\text{ext}} z) \quad (1)$$

The b_{ext} can be written as the sum of scattering and absorption by particles (b_{sp} and b_{ap}, respectively) and gases (b_{sg} and b_{ag}, respectively) and has units of inverse length:

$$b_{ext} = b_{sp} + b_{ap} + b_{sg} + b_{ag} \quad (2)$$

Visible light absorption by gases in the atmosphere is dominated by nitrogen dioxide (NO_2) and can be estimated by multiplying NO_2 concentrations by an absorption efficiency (Pitchford et al., 2007). Rayleigh scattering theory describes scattering of light by molecules (b_{sg}) and depends on the density of the atmosphere. The highest Rayleigh scattering values occur at sea level (~12 Mm^{-1} at a wavelength of 550 nm), compared to the lowest levels at high elevations (8 Mm^{-1} at ~3.0 km). Rayleigh scattering can vary due to temperature and pressure variations; it can be accurately determined if elevation and meteorological conditions are known.

Light extinction by particles depends strongly on particle size, composition, and hygroscopic properties. All particles scatter light and, if their size and refractive index are known, b_{sp} can be computed using Mie theory, assuming spherical particles. Light absorption by particles in the visible wavelengths is due to light absorbing carbon as well as some crustal mineral species. The IMPROVE algorithm was developed to estimate aerosol b_{ext} based on composition measurements and assumed size distributions and hygroscopic properties (Malm et al., 1994).

2. IMPROVE Reconstructed b_{ext} Algorithm

Total dry aerosol b_{ext} can be computed for an external mixture of aerosols by assuming a linear combination of aerosol species b_{ext} (Hand and Malm, 2007):

$$b_{ext} = \sum_j \alpha_{ext,j} M_j \quad (3)$$

where the dry species (j) mass concentration is given by M_j (μg m^{-3}), and the dry species mass extinction efficiency is given by $\alpha_{ext,j}$ (m^2 g^{-1}). Equation 3 also holds for an internally mixed

aerosol where the chemical species are mixed in fixed proportions to each other, the index of refraction is not a function of composition or size, and the aerosol density is independent of volume (Malm and Kreidenweis, 1997).

For aerosol species that absorb water, the linear relationship between total b_{ext} and M_j shown in Equation 3 will not hold because of the nonlinear behavior of aerosol hygroscopic growth on b_{ext} as a function of relative humidity (RH). To account for this effect, a humidification factor, or scattering enhancement curve ($f(RH)$), is introduced to calculate ambient (or "wet") b_{ext} as a function of RH (see Equation 4). The ratio of humidified ($b_{sp,wet}$) to dry ($b_{sp,dry}$) scattering is defined as $f(RH) = (b_{sp,wet}/b_{sp,dry})$.

$$b_{ext,wet} = \sum_j \alpha_{ext,dry,j} f(RH)_j M_{dry,j} \quad (4)$$

The third IMPROVE reconstructed b_{ext} equation (IMPROVE Equation 3, Ford et al., 2026) expanded the form of Equation 4 with several major aerosol species (Equation 5).

$$b_{ext} = 3.0 \times f_{AS}(RH) \times [\text{Ammonium Sulfate}] + 3.2 \times f_{AN}(RH) \times [\text{Ammonium Nitrate}] + 4.0 \times f_{POM}(RH) \times [\text{Particulate Organic Mass}] + 10.0 \times [\text{Elemental Carbon}] + 1.0 \times [\text{Fine Dust}] + 0.6 \times [\text{Coarse Mass}] + 1.7 \times f_{SS}(RH) \times [\text{Sea Salt}] + \text{Rayleigh Scattering} + 0.33 \times [NO_2\ (ppb)] \quad (5)$$

Ammonium sulfate mass (AS) is calculated using sulfate ion mass (1.375 × [sulfate ion]), ammonium nitrate mass (AN) using nitrate ion mass (1.29 × [nitrate mass]), and particulate organic mass (POM) using a monthly varying organic mass to organic carbon ratio and organic carbon (OC) mass (POM = [OC] × (OM/OC)) (Hand et al., 2024). Sea salt is calculated using chloride ion mass [sea salt = 1.8 × [chloride ion]). Fine dust (FD) is calculated assuming normal oxides from soil (Equation 6). Aluminum [Al], silicon [Si], calcium [Ca], iron [Fe], and titanium [Ti] mass concentrations (μg m^{-3}) are determined from $PM_{2.5}$ elemental concentrations (Hand et al., 2019).

$$FD = 2.53 \times [Al] + 2.86 \times [Si] + 1.87 \times [Ca] + 2.78 \times [Fe] + 2.23 \times [Ti] \quad (6)$$

Coarse mass (CM) is the difference between gravimetric PM_{10} and $PM_{2.5}$ mass concentrations.

The numerical values multiplied by species mass in Equation 5 are dry mass scattering efficiencies (α_{sp}) in units of $m^2\ g^{-1}$. Scattering enhancement curves ($f(RH)$) are unitless. Both α_{sp} and $f(RH)$ are calculated from assumed size distributions, composition, and for $f(RH)$, species-specific hygroscopic growth. The methods for calculating α_{sp} and $f(RH)$ are described in Sections 3 and 4, respectively.

3. Mass Scattering Efficiency

Dry α_{sp} is the amount of light scattering per dry aerosol mass and varies as a function of aerosol composition and size. Hand and Malm (2007) reviewed several methods to determine α_{sp}, including a theoretical method that relies on aerosol size distributions. The theoretical method

was used to estimate α_{sp} values in Equation 5, based on a lognormal mass median diameter (D_{pgm}) of 0.3 µm with a geometric standard deviation (σ_g) of 2.2 for AS, AN, and POM (Ford et al., 2026), and D_{pgm} of 2.5 µm and σ_g of 2.0 for sea salt (Pitchford et al., 2007). The mass size distributions ($dM/dlogD_p$) corresponding to these size parameters are shown in Figure 1 for the same initial total number of particles. The sea salt distribution is plotted on the right axis; note the difference in scales. The process for calculating theoretical b_{sp} and α_{sp} is described below. For these calculations, the dry refractive indices for AS, AN, POM, and sea salt were assumed to be 1.53, 1.55, 1.55, and 1.55, respectively. The densities for AS, AN, POM, and sea salt were assumed to be 1.77 g cm^{-3}, 1.73 g cm^{-3}, 1.4 g cm^{-3}, and 1.9 g cm^{-3}, respectively.

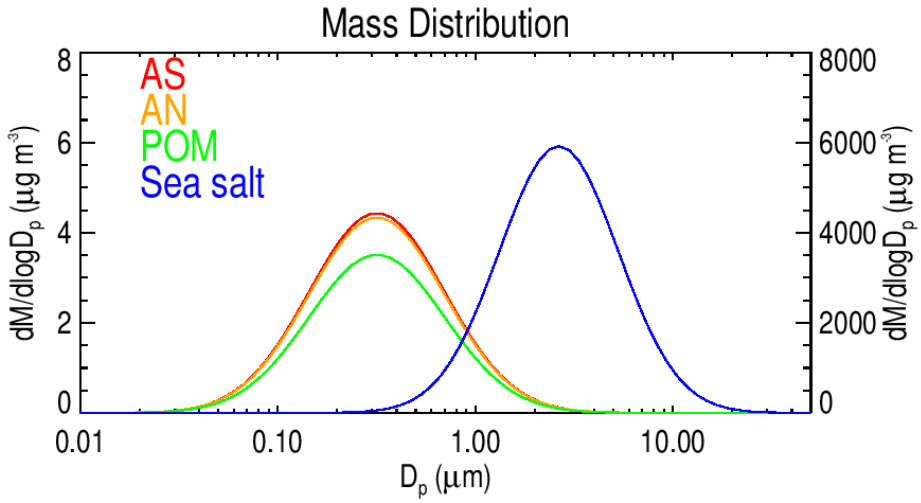

Figure 1. Mass size distributions (µg m^{-3}) for (left axis) ammonium sulfate (AS), ammonium nitrate (AN), particulate organic matter (POM), and (right axis) sea salt.

Dry Light Scattering Coefficients

Calculating b_{sp} from number size distributions ($dN/dlogDp$) is often written as Equation 7 (Seinfeld and Pandis, 1998):

$$b_{sp} = \int_0^\infty \frac{\pi}{4} D_p^2 Q_{sp} \left(\frac{dN}{dlogD_p}\right) dlogD_p \quad (7)$$

where D_p is diameter, Q_{sp} is the Mie scattering efficiency which is a function of size parameter ($x=\pi D_p/\lambda$), scattered wavelength of light, λ (550 nm), and particle refractive index. However, b_{sp} can also be calculated as a function of mass size distribution ($dM/dlogDp$) (Equation 8) by substituting for N ($M = (\pi/6) \times N \times \rho \times D_p^3$), where ρ is aerosol density. This conversion is useful if size parameters are provided for mass distributions, as they are for Equation 5.

$$b_{sp} = \int_0^\infty \frac{3}{2\rho D_p} Q_{sp} \left(\frac{dM}{dlogD_p}\right) dlogD_p \quad (8)$$

Equation 8 can also be written in a discrete form (Equation 9) where the summation occurs over the discretized form of the aerosol mass size distribution, distributed over n bins, where M_i is the mass in bin i, and $D_{pmid,i}$ is the midpoint diameter of a bin, with which the size parameter (x) is also calculated. Discretizing the lognormal mass size distribution is discussed in the next section.

$$b_{sp} = \sum_i^n \frac{3}{2\rho D_{pmid,i}} Q_{sp,i} M_i dD_p \quad (9)$$

Discretized Size Distributions

Converting a continuous aerosol lognormal size distribution into a discretized size distribution requires assumptions of the number of size distribution bins (n), and total mass, M. This process can also be applied to dry or ambient number or volume distributions. For this example, the size distribution was divided into n=100 diameter (D_p) bins, evenly spaced in $ln(D_p)$ with assumed minimum ($D_{p,min}$= 0.001 μm) and maximum diameters ($D_{p,max}$= 100 μm) and bin width of dD_p ($dD_p = (ln(D_{p,max}) - ln(D_{p,min}))/n$). Diameter limits for each bin i are calculated with Equation 10, and midpoint diameters (D_{pmid}) with Equation 11.

$$D_{p,i+1} = \exp\left(ln\left(D_{p,i}\right)\right) + dD_p \quad (10)$$

$$D_{pmid,i} = \sqrt{D_{p,i+1} \times D_{p,i}} \quad (11)$$

The mass concentration in each bin (M_i) was calculated using the difference of a cumulative distribution function, $F(D_p)$, calculated at bin diameters $D_{p,i}$ and $D_{p,i+1}$ (Seinfeld and Pandis, 1998) for total mass (M) for a given D_{pgm} and σ_g (Equation 12):

$$F\left(D_{p,i}\right) = \frac{M}{2} + \frac{M}{2} erf\left(\frac{\ln\left({D_{p,i}}/{D_{pgm}}\right)}{\sqrt{2} ln(\sigma_g)}\right) \quad (12)$$

The bin mass concentration, M_i, is determined from Equation 13.

$$M_i = F(D_{p,i} + 1) - F(D_{p,i}) \quad (13)$$

M_i from Equation 13 and $D_{pmid,i}$ from Equation 11 can be used in Equation 9 to calculate b_{sp}.

Dry Mass Scattering Efficiency

Dry α_{sp} is calculated as the ratio of dry b_{sp} (Equation 9) to total dry M, summed over the entire size distribution (Equation 14).

$$\alpha_{sp,dry} = b_{sp,dry}/M_{dry} \quad (14)$$

4. Hygroscopic Growth

The scattering enhancement curves applied in Equation 5 were calculated assuming species-specific particle hygroscopic growth. Hygroscopic diameter growth curves *(DDo*), or the ratio of "wet" to "dry" diameter as a function of RH, were calculated using the kappa (κ) water uptake framework following Equation 15.

$$DDo = \left(\frac{\kappa}{\frac{1}{RH/100}-1}+1\right)^{1/3} \quad (15)$$

Values of κ used were 0.61, 0.67, 0.1, and 1.1 for AS, AN, POM, and SS, respectively (Petters and Kreidenweis, 2007; Zieger et al. 2017). The resulting *DDo* curves for each species are shown in Figure 2 and provided in Table 1.

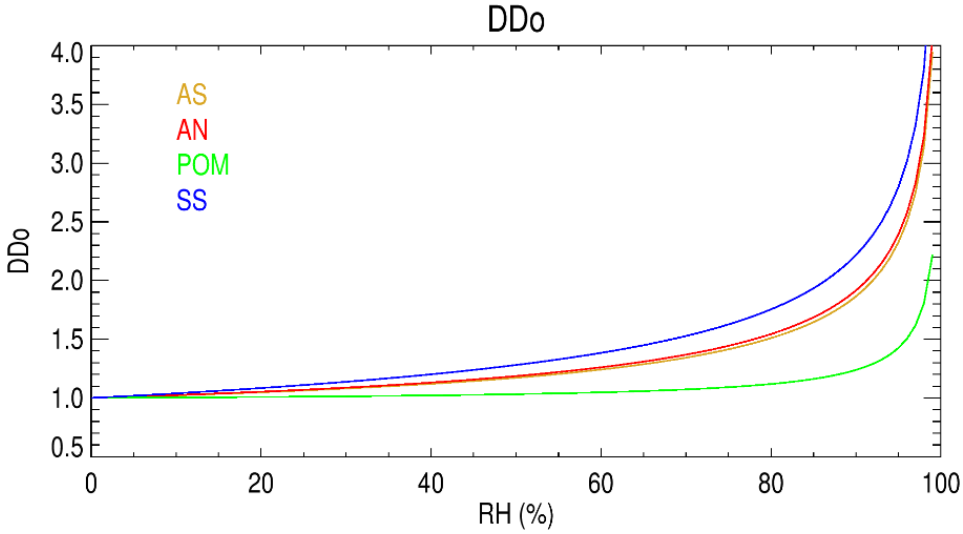

Figure 2. Particle diameter growth curves (*DDo*) for ammonium sulfate (AS), ammonium nitrate (AN), particulate organic matter (POM), and sea salt (SS), as a function of relative humidity (RH).

As defined earlier, *f(RH)* is the ratio of wet to dry b_{sp} as a function of RH. Dry b_{sp} ($b_{sp,dry}$) was calculated with Equation 9. Wet b_{sp} ($b_{sp,wet}$) can be calculated by substituting wet parameters into Equation 9, as shown in Equation 16,

$$b_{sp,wet} = \sum_i^n \frac{3}{2\rho_{wet} D_{pmid,wet,i}} Q_{sp,wet,i} M_{wet,i} dD_p \quad (16)$$

However, Equation 16 can be simplified to Equation 17 with several substitutions following Hand et al. (2010).

$$b_{sp,wet} = \sum_i^n \frac{3}{2\rho_{dry} D_{pmid,dry,i}} Q_{sp,wet,i} DDo^2 M_{dry,i} dD_p \quad (17)$$

The substitutions were performed in the following way. M_{wet} can be substituted using DDo as shown in Equations 18-20.

$$\frac{M_{wet}}{M_{dry}} = \frac{\rho_{wet} V_{wet}}{\rho_{dry} V_{dry}} \quad (18)$$

Substituting V as $(\pi/6) \times D^3$ gives Equation 19.

$$\frac{M_{wet}}{M_{dry}} = \frac{\rho_{wet}\left(\frac{\pi}{6} D_{wet}^3\right)}{\rho_{dry}\left(\frac{\pi}{6} D_{dry}^3\right)} \quad (19)$$

Finally, substituting DDo for D_{wet}/D_{dry} gives Equation 20.

$$M_{wet} = M_{dry} \frac{\rho_{wet}}{\rho_{dry}} DDo^3 \quad (20)$$

Substituting this definition of M_{wet} into Equation 16 allows us to derive Equation 17. A wet size parameter was calculated as $x_{wet}=\pi D_{pmid,dry} \times DDo/\lambda$ and the wet Mie extinction efficiency ($Q_{sp,wet}$) was calculated using a wet refractive index (m_{wet}), which was calculated using Equations 21-23.

Refractive Index

Refractive index (m) corresponding to a mixture can be calculated based on the volume-weighted method (Ouimette and Flagan, 1982; Hasan and Dzubay, 1983):

$$m = \sum_i \frac{V_i}{V} m_i \quad (21)$$

where the component volume is given by V_i, and the mixture (or total) volume is given by V and the component refractive index by m_i. For wet refractive index the two components are the dry aerosol mass and water:

$$m_{wet} = \frac{V_{dry}}{V_{wet}} m_{dry} + \frac{V_{wat}}{V_{wet}} m_{wat} \quad (22)$$

The volume of water (V_{wat}) can be written as $V_{wat} = V_{wet} - V_{dry}$ and $V = (\pi/6) \times D^3$. Substituting these into Equation 22 and multiplying the numerator and denominator by D_{dry}^{-3} gives Equation 23.

$$m_{wet} = \frac{m_{dry} + m_{wat}(DDo^3 - 1)}{DDo^3} \quad (23)$$

Using these wet parameters in Equation 17 allows $b_{sp,wet}$ to be calculated as a function of RH. The $f(RH)$ curve is then taken as the ratio of $b_{sp,wet}$ to $b_{sp,dry}$. The $f(RH)$ curves for POM, AS, and AN in Equation 5 are shown in Figure 3 and provided in Table 2.

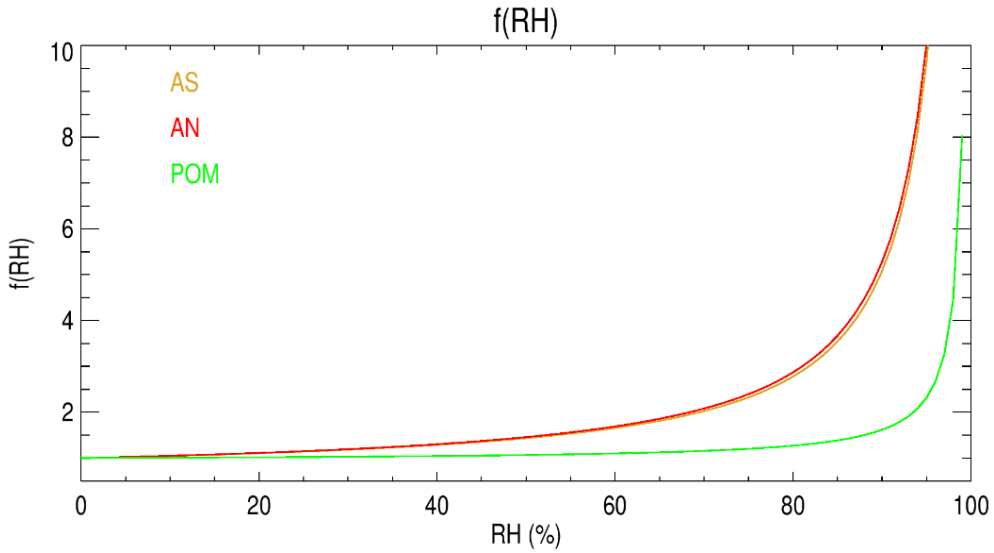

Figure 3. Scattering enhancement (*f(RH)*) curves for ammonium sulfate (AS), ammonium nitrate (AN) and particulate organic matter (POM) as a function of relative humidity (RH), corresponding to a wavelength of 550 nm.

Although wet density (ρ_{wet}) was not needed in the previous formulation, its derivation is included here for completeness.

Density

Wet density (ρ_{wet}) is derived using Equations 24-27. To begin, M_{wet} can be written as the sum of dry (M_{dry}) and water mass (M_{wat}). Substituting the definition of mass as $V \times \rho$, and the water volume (V_{wat}) as V_{wet}-V_{dry}, M_{wet} can be written as Equation 24.

$$M_{wet} = V_{dry} \times \rho_{dry} + (V_{wet} - V_{dry}) \times \rho_{wat} \quad (24)$$

Substituting $(\pi/6) \times D^3$ for V gives Equation 25:

$$\frac{\pi}{6} D_{wet}^3 \rho_{wet} = \frac{\pi}{6} D_{dry}^3 \rho_{dry} + \left(\frac{\pi}{6} D_{wet}^3 - \frac{\pi}{6} D_{dry}^3\right) \rho_{wat} \quad (25)$$

Simplifying gives Equation 26:

$$\rho_{wet} = \frac{D_{dry}^3 \rho_{dry} + (D_{wet}^3 - D_{dry}^3)\rho_{wat}}{D_{wet}^3} \quad (26)$$

Multiplying the numerator and denominator by D_{dry}^{-3}, and substituting DDo^3 for $(D_{wet}/D_{dry})^3$ gives Equation 27:

$$\rho_{wet} = \frac{\rho_{dry} + \rho_{wat}(DDo^3 - 1)}{DDo^3} \quad (27)$$

5. Cyclone Efficiency and Derived Optical Properties

The IMPROVE sampler operates three modules with a 2.5 µm cyclone, which partitions the sampled aerosol such that particles with aerodynamic diameters less than 2.5 µm are collected. A cyclone efficiency curve (*E(Dp)*) is characterized by Equation 28 (Winklmayr et al., 1990):

$$E(D_p) = \left(1 + \left(\frac{D_{50}}{D_p}\right)^{2s}\right)^{-1} \quad (28)$$

where D_{50} is the aerodynamic diameter (2.5 µm) corresponding to the cyclone and D_p is particle diameter. The slope, s, is the square root of the particle diameter ratio for the inlet penetration at 16% and 84%. The IMPROVE sampler uses an AIHL-type cyclone with a slope of 1.16 (Solomon et al., 2014). However, a study of the IMPROVE cyclone (Turner et al., 2006) suggests the efficiency curve may be sharper. Figure 4 shows a penetration curve ($P(D_p) = 1-E(D_p)$), corresponding to the particles collected on the filter, with an example mass size distribution with an aerodynamic D_{pgm} of 2.5 µm and of σ_g of 2.0. The original size distribution is in blue, and the "collected" size distribution is in red. An idealized (perfect) penetration efficiency is shown as a vertical black line. An idealized cyclone would not allow the collection of any particles with aerodynamic diameters greater than 2.5 µm, but given the shape of the actual penetration curve, a portion of the mass distribution above 2.5 µm is collected. For the ideal cut point example, half of the original mass is collected on the filter.

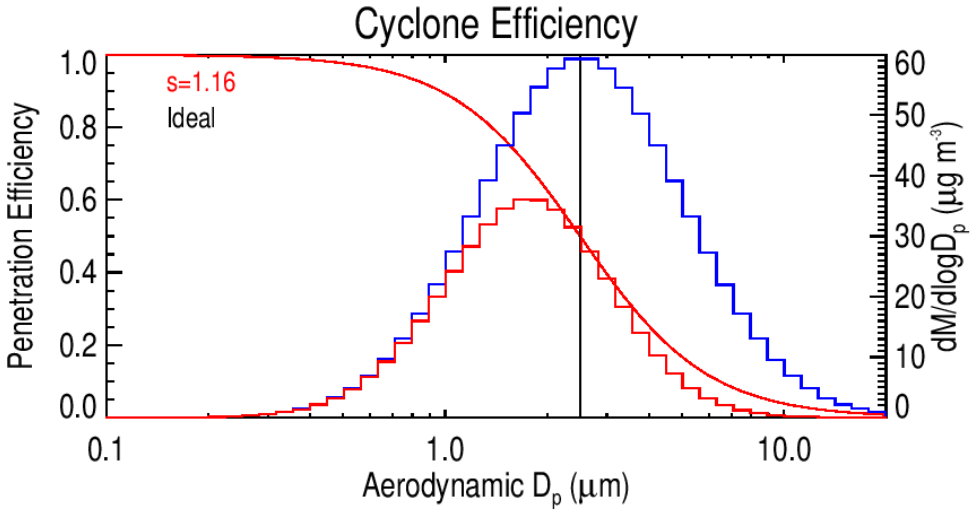

Figure 4. Penetration efficiency (smooth red curve) for the IMPROVE 2.5 µm cyclone with a slope of 1.16 and an idealized penetration efficiency in black. The blue mass size distribution is the original, and the red is the "collected" size distribution after applying the penetration efficiency.

The cyclone efficiency therefore determines the derived α_{sp} for sea salt aerosol collected on the $PM_{2.5}$ filter (Hand and Malm, 2007). The b_{sp} corresponding to the fraction of sea salt not collected on the $PM_{2.5}$ filter is accounted for in the coarse mass b_{sp}.

When applying the cyclone penetration curve to the size distributions (and total mass) used in Equations 9 and 17 to calculate $b_{sp,dry}$ and $b_{sp,wet}$, the binned mass (M_i) is multiplied by the penetration curve before calculating $b_{sp,dry}$ or $b_{sp,wet}$. The penetration curve was first converted to geometric (physical) diameter by calculating a geometric D_{50} ($D_{50,geo}$) using Equation 28 because Mie theory is applied using physical (not aerodynamic) size.

$$D_{50,geo} \sim D_{50} \sqrt{\frac{\chi \rho_o}{\rho}} \tag{28}$$

where the particle shape factor is χ and was assumed to be one, and ρ_o corresponds to the reference density (1 g cm^{-3}).

The dry α_{sp} can be calculated using Equation 14 with b_{sp} and M calculated after applying a penetration curve. For sea salt (with size parameters and properties listed earlier), an initial dry α_{sp} of 1.7 m^2 g^{-1} was derived after applying the cyclone curve, which is the value used in Equation 5. For the case with no cyclone, a lower value of 1.1 m^2 g^{-1} was derived because more large particles were included in the calculation (see Figures 5a and 5b for dry SS α_{sp} calculated with and without a cyclone, respectively, as a function of a range of lognormal size distributions with varying geometric D_{pgm} and σ_g). The major differences between the curves in Figure 5a and 5b occur for size distributions with larger D_{pgm} closer to the size range where the cyclone has a bigger impact. This cyclone effect does not impact the AS, AN, and POM α_{sp} values because their size distribution parameters are small enough to not conflict with the cyclone penetration curves.

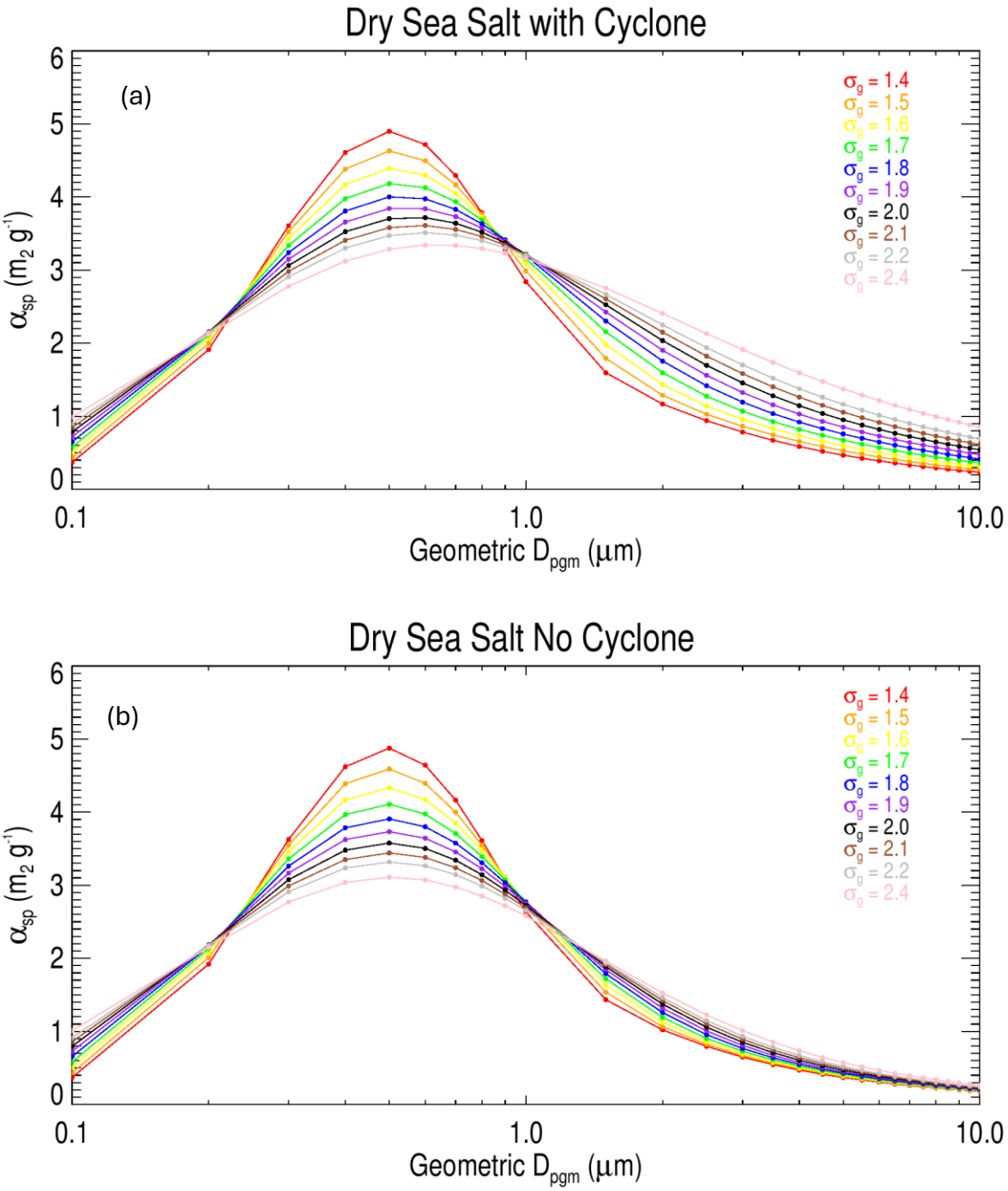

Figure 5. Dry sea salt mass scattering efficiency, α_{sp} (m^2 g^{-1}), as a function of geometric mass median diameter (D_{pgm}) and geometric standard deviation (σ_g) after applying (a) an IMPROVE cyclone and (b) no cyclone. Values correspond to a wavelength of 550 nm.

Sea Salt Scattering Enhancement Curves (f(RH))

The *f(RH)* for sea salt calculated with and without a cyclone is shown in Figure 6. The $b_{sp,dry}$ and $b_{sp,wet}$ were calculated using Equations 9 and 17, respectively. There is minimal difference between the two curves. The *f(RH)* curve for sea salt included in Equation 5 was calculated with a $PM_{2.5}$ cyclone; the corresponding values of *DDo* and *f(RH)* for sea salt are included in Table 1 and Table 2, respectively.

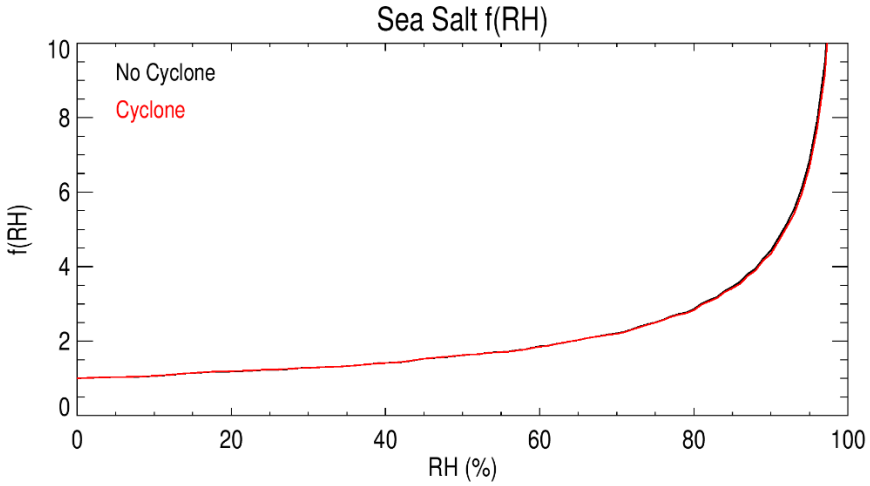

Figure 6. *f(RH)* for sea salt calculated with and without a cyclone.

6. Fine Dust and Coarse Mass Scattering Efficiency

The values of α_{sp} for FD and CM in Equation 5 originated from a study in the California desert (Trijonis and Pitchford, 1987); the α_{sp} for FD was determined by a regression analysis and literature review, while the α_{sp} for CM was determined from the ratio of measured coarse b_{sp} and CM.

7. References

Ford, B., A. J. Prenni, W. Malm, S. A. Copeland, B. A. Schichtel, and J. Hand (2026), Analysis and updates to the IMPROVE Equation for estimating light extinction, *Journal of the Air & Waste Management Association*, https://doi.org/10.1080/10962247.2026.2651554.

Hand, J. L., D. E. Day, G. M. McMeeking, E. J. T. Levin, C. M. Carrico, S. M. Kreidenweis, W. C. Malm, A. Laskin, and Y. Desyaterik (2010), Measured and modeled humidification factors of fresh smoke particles from biomass burning: role of inorganic constituents, *Atmospheric Chemistry and Physics*, *10*(13), 6179-6194, https://doi.org/10.5194/acp-10-6179-2010.

Hand, J. L., and W. C. Malm (2007), Review of aerosol mass scattering efficiencies from ground-based measurements since 1990, *Journal of Geophysical Research: Atmospheres*, *112*(D16), https://doi.org/10.1029/2007JD008484.

Hand, J. L., A. J. Prenni, S. M. Raffuse, N. P. Hyslop, W. C. Malm, and B. A. Schichtel (2024), Spatial and Seasonal Variability of Remote and Urban Speciated Fine Particulate Matter in the United States, *Journal of Geophysical Research: Atmospheres*, *129*(23), e2024JD042579, https://doi.org/10.1029/2024JD042579.

Hand, J. L., A. J. Prenni, B. A. Schichtel, W. C. Malm, and J. C. Chow (2019), Trends in remote PM2.5 residual mass across the United States: Implications for aerosol mass reconstruction in the IMPROVE network, *Atmospheric Environment*, *203*, 141-152, https://doi.org/10.1016/j.atmosenv.2019.01.049.

Hasan, H., and T. G. Dzubay (1983), Apportioning light extinction coefficients to chemical species in atmospheric aerosol, *Atmospheric Environment (1967)*, *17*(8), 1573-1581, https://doi.org/10.1016/0004-6981(83)90310-4.

Malm, W. C., and S. M. Kreidenweis (1997), The effects of models of aerosol hygroscopicity on the apportionment of extinction, *Atmospheric Environment*, *31*(13), 1965-1976, https://doi.org/10.1016/S1352-2310(96)00355-X.

Malm, W. C., J. F. Sisler, D. Huffman, R. A. Eldred, and T. A. Cahill (1994), Spatial and seasonal trends in particle concentration and optical extinction in the United States, *Journal of Geophysical Research: Atmospheres*, *99*(D1), 1347-1370, https://doi.org/10.1029/93JD02916.

Seinfeld, J. H. and S. N. Pandis (1998), Atmospheric Chemistry and Physics: From Air Pollution to Climate Change, Ed: John Wiley and Sons, pp 423 & 1125.

Ouimette, J. R. and R. C. Flagan (1982), The extinction coefficient of multicomponent aerosols, *Atmospheric Environment (1967), 16*(10), 2405-2419, https://doi.org/10.1016/0004-6981(82)90131-7.

Petters, M. D., and S. M. Kreidenweis (2007), A single parameter representation of hygroscopic growth and cloud condensation nucleus activity, *Atmospheric Chemistry and Physics*, *7*(8), 1961-1971, https://doi.org/10.5194/acp-7-1961-2007.

Pitchford, M., W. C. Malm, B. A. Schichtel, N. Kumar, D. Lowenthal, and J. L. Hand (2007), Revised algorithm for estimating light extinction from IMPROVE particle speciation data, *Journal of the Air & Waste Management Association*, *57*(11), 1326-1336, https://doi.org/10.3155/1047-3289.57.11.1326.

Solomon, P. A., D. Crumpler, J. B. Flanagan, R. K. M. Jayanty, E. E. Rickman, and C. E. McDade (2014), U.S. National PM2.5 Chemical speciation monitoring networks—CSN and IMPROVE: Description of networks, *Journal of the Air & Waste Management Association*, *64*(12), 1410-1438, https://doi.org/10.1080/10962247.2014.956904.

Turner, J. R., N. Kreisberg, G. F. Walsh, and S. V. Hering (2006), Aerosol penetration characteristics of the Interagency Monitoring of Protected Visual Environments (IMPROVE)

sampler PM2.5 cyclone, https://improvevisibility.org/docs/Publications/GrayLit/045_Cyclone%20efficiency/Turner_Cyclone_2006IAC_060130.pdf

Trijonis, J. C. and M. Pitchford (1987), Preliminary Extinction Budget Results from the RESOLVE program, edited by P. S. Bhardwaja, Visibility Protection Research and Policy Aspects, Air Pollution Control Association, Pittsburgh, PA.

Winklmayr, W., H.-C. Wang, and W. John (1990), Adaptation of the Twomey Algorithm to the Inversion of Cascade Impactor Data, *Aerosol Science and Technology*, *13*(3), 322-331, https://doi.org/10.1080/02786829008959448.

Zieger, P., et al. (2017), Revising the hygroscopicity of inorganic sea salt particles, *Nature Commununications*, *8*(1), 15883, https://doi.org/10.1038/ncomms15883.

Tables

Table 1. Hygroscopic growth factors, DDo, for ammonium sulfate (AS), ammonium nitrate (AN), particulate organic matter (POM), and sea salt (SS), as a function of relative humidity (RH).

RH (%)	AS DDo	AN DDo	POM DDo	SS DDo	RH (%)	AS DDo	AN DDo	POM DDo	SS DDo
0	1.0000	1.0000	1.0000	1.0000	50	1.1720	1.1864	1.0323	1.2806
1	1.0020	1.0023	1.0003	1.0037	51	1.1780	1.1929	1.0336	1.2896
2	1.0041	1.0045	1.0007	1.0074	52	1.1842	1.1995	1.0349	1.2989
3	1.0062	1.0069	1.0010	1.0112	53	1.1906	1.2063	1.0363	1.3085
4	1.0084	1.0092	1.0014	1.0151	54	1.1972	1.2134	1.0377	1.3183
5	1.0106	1.0116	1.0018	1.0189	55	1.2041	1.2207	1.0392	1.3285
6	1.0128	1.0141	1.0021	1.0229	56	1.2111	1.2282	1.0407	1.3389
7	1.0151	1.0165	1.0025	1.0269	57	1.2184	1.2360	1.0424	1.3496
8	1.0174	1.0191	1.0029	1.0309	58	1.2259	1.2440	1.0441	1.3606
9	1.0197	1.0216	1.0033	1.0350	59	1.2337	1.2523	1.0458	1.3721
10	1.0221	1.0242	1.0037	1.0392	60	1.2418	1.2610	1.0477	1.3838
11	1.0245	1.0269	1.0041	1.0434	61	1.2502	1.2699	1.0496	1.3960
12	1.0270	1.0296	1.0045	1.0477	62	1.2589	1.2792	1.0517	1.4086
13	1.0295	1.0323	1.0050	1.0520	63	1.2680	1.2888	1.0538	1.4216
14	1.0321	1.0351	1.0054	1.0564	64	1.2774	1.2988	1.0561	1.4351
15	1.0347	1.0380	1.0058	1.0609	65	1.2872	1.3093	1.0584	1.4491

16	1.0373	1.0408	1.0063	1.0655	66	1.2975	1.3201	1.0609	1.4636
17	1.0400	1.0438	1.0068	1.0701	67	1.3081	1.3314	1.0636	1.4787
18	1.0428	1.0468	1.0073	1.0748	68	1.3193	1.3433	1.0663	1.4944
19	1.0456	1.0499	1.0078	1.0795	69	1.3310	1.3556	1.0693	1.5108
20	1.0484	1.0530	1.0083	1.0844	70	1.3432	1.3686	1.0724	1.5279
21	1.0514	1.0562	1.0088	1.0893	71	1.3560	1.3821	1.0757	1.5457
22	1.0543	1.0594	1.0093	1.0943	72	1.3695	1.3964	1.0793	1.5644
23	1.0574	1.0627	1.0099	1.0993	73	1.3837	1.4114	1.0830	1.5840
24	1.0605	1.0661	1.0104	1.1045	74	1.3987	1.4272	1.0871	1.6045
25	1.0636	1.0695	1.0110	1.1097	75	1.4145	1.4439	1.0914	1.6261
26	1.0669	1.0730	1.0116	1.1151	76	1.4312	1.4615	1.0960	1.6489
27	1.0702	1.0766	1.0122	1.1205	77	1.4490	1.4802	1.1010	1.6730
28	1.0735	1.0802	1.0128	1.1260	78	1.4679	1.5001	1.1064	1.6985
29	1.0770	1.0840	1.0134	1.1317	79	1.4880	1.5212	1.1123	1.7256
30	1.0805	1.0878	1.0141	1.1374	80	1.5096	1.5439	1.1187	1.7544
31	1.0841	1.0917	1.0148	1.1432	81	1.5327	1.5682	1.1257	1.7852
32	1.0878	1.0957	1.0154	1.1492	82	1.5576	1.5943	1.1333	1.8182
33	1.0915	1.0997	1.0162	1.1552	83	1.5845	1.6225	1.1417	1.8538
34	1.0954	1.1039	1.0169	1.1614	84	1.6137	1.6531	1.1510	1.8922
35	1.0993	1.1081	1.0176	1.1677	85	1.6456	1.6865	1.1614	1.9340
36	1.1033	1.1125	1.0184	1.1742	86	1.6807	1.7231	1.1731	1.9796
37	1.1075	1.1170	1.0192	1.1807	87	1.7193	1.7634	1.1862	2.0297
38	1.1117	1.1215	1.0200	1.1874	88	1.7623	1.8083	1.2012	2.0852
39	1.1160	1.1262	1.0209	1.1942	89	1.8106	1.8587	1.2185	2.1472
40	1.1205	1.1310	1.0217	1.2012	90	1.8653	1.9157	1.2386	2.2172
41	1.1250	1.1359	1.0226	1.2084	91	1.9281	1.9810	1.2622	2.2972
42	1.1297	1.1409	1.0236	1.2157	92	2.0012	2.0571	1.2907	2.3899
43	1.1345	1.1461	1.0245	1.2231	93	2.0881	2.1473	1.3254	2.4994
44	1.1394	1.1514	1.0255	1.2308	94	2.1937	2.2570	1.3692	2.6320
45	1.1445	1.1568	1.0266	1.2386	95	2.3264	2.3945	1.4260	2.7978
46	1.1497	1.1624	1.0276	1.2466	96	2.5008	2.5753	1.5037	3.0147
47	1.1550	1.1682	1.0287	1.2547	97	2.7468	2.8299	1.6177	3.3192
48	1.1605	1.1741	1.0299	1.2631	98	3.1377	3.2342	1.8070	3.8006
49	1.1662	1.1802	1.0311	1.2718	99	3.9449	4.0682	2.2172	4.7900

Table 2. *f(RH)* values for ammonium sulfate (AS), ammonium nitrate (AN), particulate organic matter (POM), and sea salt (SS) as a function of RH.

RH (%)	$f_{POM}(RH)$	$f_{AS}(RH)$	$f_{AN}(RH)$	$f_{ss}(RH)$	RH (%)	$f_{POM}(RH)$	$f_{AS}(RH)$	$f_{AN}(RH)$	$f_{ss}(RH)$
0	1.0000	1.0002	1.0000	1.0000	50	1.0662	1.4340	1.4565	1.6207
1	1.0006	1.0045	1.0047	1.0017	51	1.0690	1.4522	1.4756	1.6400
2	1.0014	1.0088	1.0092	1.0050	52	1.0720	1.4708	1.4953	1.6628
3	1.0021	1.0131	1.0136	1.0106	53	1.0748	1.4904	1.5161	1.6838
4	1.0027	1.0179	1.0183	1.0152	54	1.0779	1.5109	1.5374	1.7044
5	1.0034	1.0224	1.0232	1.0219	55	1.0812	1.5323	1.5601	1.7286
6	1.0041	1.0272	1.0281	1.0307	56	1.0847	1.5547	1.5839	1.7573
7	1.0049	1.0323	1.0335	1.0502	57	1.0883	1.5784	1.6087	1.7842
8	1.0057	1.0370	1.0387	1.0497	58	1.0921	1.6029	1.6341	1.8031
9	1.0065	1.0421	1.0441	1.0589	59	1.0958	1.6286	1.6617	1.8265
10	1.0072	1.0473	1.0495	1.0709	60	1.1001	1.6552	1.6898	1.8526
11	1.0081	1.0529	1.0551	1.0847	61	1.1043	1.6840	1.7198	1.8825
12	1.0089	1.0581	1.0605	1.0982	62	1.1090	1.7140	1.7518	1.9177
13	1.0098	1.0636	1.0666	1.1110	63	1.1138	1.7454	1.7845	1.9575
14	1.0106	1.0695	1.0726	1.1139	64	1.1188	1.7788	1.8201	1.9916
15	1.0116	1.0752	1.0785	1.1207	65	1.1242	1.8134	1.8572	2.0188
16	1.0125	1.0811	1.0848	1.1294	66	1.1296	1.8508	1.8964	2.0533
17	1.0134	1.0875	1.0916	1.1389	67	1.1358	1.8905	1.9378	2.0930
18	1.0144	1.0937	1.0983	1.1492	68	1.1421	1.9329	1.9824	2.1338
19	1.0154	1.1003	1.1049	1.1602	69	1.1489	1.9778	2.0297	2.1840
20	1.0164	1.1069	1.1119	1.1722	70	1.1563	2.0258	2.0803	2.2260
21	1.0174	1.1137	1.1191	1.1860	71	1.1641	2.0772	2.1344	2.2745
22	1.0184	1.1207	1.1264	1.2003	72	1.1725	2.1326	2.1925	2.3286
23	1.0196	1.1278	1.1339	1.2086	73	1.1815	2.1916	2.2548	2.3907
24	1.0207	1.1352	1.1417	1.2162	74	1.1913	2.2554	2.3222	2.4530
25	1.0220	1.1428	1.1497	1.2299	75	1.2017	2.3246	2.3949	2.5168
26	1.0232	1.1505	1.1579	1.2325	76	1.2132	2.3997	2.4736	2.5832
27	1.0243	1.1584	1.1662	1.2425	77	1.2254	2.4815	2.5590	2.6642
28	1.0256	1.1665	1.1749	1.2522	78	1.2389	2.5710	2.6528	2.7425
29	1.0268	1.1750	1.1839	1.2638	79	1.2535	2.6701	2.7565	2.8142
30	1.0283	1.1836	1.1933	1.2780	80	1.2698	2.7782	2.8700	2.8941
31	1.0295	1.1930	1.2027	1.2930	81	1.2878	2.8983	2.9958	2.9743
32	1.0309	1.2023	1.2125	1.3115	82	1.3078	3.0319	3.1363	3.0677
33	1.0324	1.2117	1.2222	1.3326	83	1.3303	3.1816	3.2933	3.1713
34	1.0341	1.2213	1.2327	1.3464	84	1.3558	3.3506	3.4709	3.2885
35	1.0354	1.2317	1.2434	1.3599	85	1.3850	3.5422	3.6713	3.4343

36	1.0372	1.2421	1.2540	1.3720	86	1.4176	3.7611	3.9018	3.5875
37	1.0387	1.2530	1.2657	1.3868	87	1.4558	4.0146	4.1669	3.7470
38	1.0404	1.2639	1.2774	1.4007	88	1.5003	4.3094	4.4749	3.9391
39	1.0423	1.2756	1.2892	1.4195	89	1.5533	4.6583	4.8397	4.1623
40	1.0441	1.2875	1.3017	1.4353	90	1.6166	5.0776	5.2778	4.4255
41	1.0460	1.3000	1.3152	1.4521	91	1.6940	5.5893	5.8121	4.7544
42	1.0478	1.3130	1.3287	1.4673	92	1.7908	6.2270	6.4783	5.1168
43	1.0498	1.3264	1.3427	1.4808	93	1.9155	7.0441	7.3306	5.5596
44	1.0519	1.3397	1.3568	1.4973	94	2.0821	8.1296	8.4590	6.1422
45	1.0543	1.3540	1.3723	1.5164	95	2.3167	9.6327	10.0224	6.8634
46	1.0563	1.3687	1.3876	1.5347	96	2.6704	11.8526	12.3260	7.8899
47	1.0587	1.3844	1.4038	1.5542	97	3.2660	15.4551	16.0589	9.4725
48	1.0611	1.4004	1.4206	1.5770	98	4.4649	22.3343	23.1564	12.3010
49	1.0638	1.4166	1.4383	1.6021	99	8.0374	40.9367	42.2520	19.2701